Author/s:
Wang, Y;Yao, H;Zhou, J;Hong, Y;Chen, B;Zhang, B;Smith, TA;Wong, WWH;Zhao, Z

Title:
A water-soluble, AIE-active polyelectrolyte for conventional and fluorescence lifetime imaging of mouse neuroblastoma neuro-2A cells

Date:
2018-03-15

Citation:
Wang, Y., Yao, H., Zhou, J., Hong, Y., Chen, B., Zhang, B., Smith, T. A., Wong, W. W. H. & Zhao, Z. (2018). A water-soluble, AIE-active polyelectrolyte for conventional and fluorescence lifetime imaging of mouse neuroblastoma neuro-2A cells. Journal of Polymer Science Part A Polymer Chemistry, 56 (6), pp.672-680. https://doi.org/10.1002/pola.28943.

Journal Name

COMMUNICATION

A water-soluble, AIE-active polyelectrolyte for conventional and fluorescence lifetime imaging of mouse neuroblastoma neuro-2A cells

Received 00th January 20xx,
Accepted 00th January 20xx,

DOI: 10.1039/x0xx00000x

www.rsc.org/

Jian Zhou,[*a,c] Yinan Wang,[a] Yuning Hong,[c,d] Bin Chen,[b] Mengxia Gao,[a] Bolong Zhang,[c] Trevor A. Smith,[*c] Wallace W. H. Wong,[c] and Zujin Zhao[*b]

A new conjugated polyelectrolyte containing tetraphenylethene units in the backbone is synthesized and characterized. This polyelectrolyte is water-soluble and exhibits aggregation-induced emission (AIE) behaviour. It is biocompatible and can be directly used in conventional and fluorescence lifetime imaging of mouse neuroblastoma neuro-2A cells, providing useful information of cellular morphology and intracellular aggregation or motion.

Conjugated polyelectrolytes (CPEs) comprised of π-electron delocalized backbones and water-soluble side chains have demonstrated great potential applications in chemical and biological sensing[1,2] of various analytes including proteins,[3-5] enzymes,[6-8] DNA,[9,10] and metal ions.[11,12] Owing to their prominent properties, such as high photobleaching resistance, excellent aqueous stability and good biocompatibility, CPEs have been further explored as promising light-activated cellular probes for bioimaging.[13-15] By taking advantage of the electrostatic interaction between CPEs and oppositely charged cells, fluorescent CPEs can easily enter cells for long-term tracking of activities in cells, such as apoptotic process,[16] or generate reactive oxygen species to kill cancer cells.[17-19] However, on account of their inherently amphiphilic structures (hydrophobic backbone and hydrophilic side groups), CPEs have a strong tendency to aggregate in aqueous solution or polar organic solvents, and as a result when they tag proteins within the cells and aggregate strongly, their fluorescence intensity decreases and the emission peak appears as a broad, structureless band, which is red-shifted significantly from its original position in good solvents.[20] Furthermore, compared with the quenching effect for a monomeric model small molecule, CPEs show considerably larger quenching effect, suggesting that the quenching response is amplified in the polymers.[21] Therefore, traditional CPE-based fluorescent cellular probes mainly operate in a "turn-off" mode. To alleviate the aggregation-caused quenching effect, the CPEs with a hyperbranched architecture, which can self-assemble to form core-shell nanoparticles in aqueous media, have been studied in recent years. These nanoparticles possess well-controlled size and display higher photostability for efficient bioconjugation and specific cellular imaging.[13,22,23]

In recent decades, a novel class of fluorogenic molecules with aggregation-induced emission (AIE) characteristics has sparked enthusiastic research in the design and synthesis of probes for bioimaging applications.[24,25] AIE fluorogens (AIEgens) are nearly non-emissive in the molecularly dispersed state, however, upon aggregating, intramolecular rotation of aromatic rings is restricted and the non-radiative decay channel is blocked, allowing molecules to emit strong fluorescence. Compared with conventional dyes, AIEgens show merits of high brightness, low background signal and good photostability. These superior features enable AIEgens to function as efficient probes in real-time, on-site and non-invasive visualization of biological molecules, live cells and organisms.[26-30] Whereas noteworthy advances have been achieved regarding small molecular AIE probes, macromolecular AIE probes have been less explored. Macromolecular AIE probes succeed in maintaining many CPE merits including superb physical stability, flexible synthesis, long-term cell tracking, photobleaching resistance, etc.[31-34]

Most fluorescence measurements in cells and tissues are normally made by monitoring relative emission intensity using calibration standards or by self-referencing. Unlike fluorescence intensity-based measurements, time-resolved fluorescence imaging is less affected by experimental conditions such as scattered light or fluorophore concentration.[35,36] Fluorescence lifetimes can be sensitive to a great variety of internal factors defined by the fluorophore structure and external factors including temperature, polarity, viscosity and the presence of fluorescence quenchers. A combination of environmental sensitivity and parametric independence mentioned above renders time-resolved fluorescence measurements a separate yet complementary method to traditional fluorescence intensity measurements.[37] Therefore,

Commented [WW1]: At this point, you may want to discuss a bit more about the literature and state what are the challenges and problems with published AIE-CPE systems. You can also talk about your previous work in Polymer Chemistry here.

[a] College of Material, Chemistry and Chemical Engineering, Hangzhou Normal University, Hangzhou 310036, China. Email: zhoujian@hznu.edu.cn
[b] State Key Laboratory of Luminescent Materials and Devices, South China University of Technology, Guangzhou 510640, China. Email: mszjzhao@scut.edu.cn
[c] School of Chemistry, The University of Melbourne, Victoria 3010, Australia. Email: trevoras@unimelb.edu.au
[d] Department of Chemistry and Physics, La Trobe University, Victoria 3086, Australia.

† Electronic Supplementary Information (ESI) available: Experimental, absorption spectrum of P1, fluorescence decay of P1, and ^{1}H and ^{13}C NMR spectra. See DOI: 10.1039/x0xx00000x

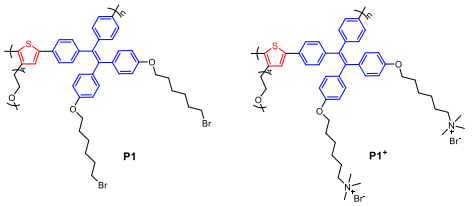

Scheme 1. Molecular structures of 4,4'-(2,2-diphenylethene-1,1-diyl)bis((alkyloxy)benzene) -based copolymers P1 and P1$^+$.

fluorescence lifetime-based spectroscopy or microscopy technqiues have already been applied in measurements of graphene quantum dots,[38] light-emitting conjugated polymeric films,[39] the kinetics of α-chymotrypsin hydrolyzing,[40] imaging of molecular probes in cells and so forth.[36,41,42] The first work in which living cells stained with AIE small molecules have been imaged using the fluorescence lifetime-based measurement, and provided intracellular viscosity sensing.[43]

In this work, to combine the merits of CPEs and AIEgens, we directly copolymerized a tetraphenylethene (TPE)-based AIEgen with a thiophene-based monomer containing a hydrophilic ether linkage to afford a water-soluble linear CPE with AIE groups in the backbone. The new fluorescent CPE displays AIE characteristics with green emission. The utility as a bioprobe for detection of mouse neuroblastoma neuro-2A cells is investigated through Confocal Laser Scanning Microscopy (CLSM) and Time Correlated Single Photon Counting (TCSPC) based fluorescence lifetime imaging (FLIM). This macromolecular AIE bioprobe can enter living cells in a noninvasive manner, and emit bright fluorescence with low cytotoxicity. The fluorescence lifetime-based microscopy based on this probe provides a full map of cellular morphology and molecular motion under various experimental conditions.

Scheme 1 illustrates the molecular structure of CPE (P1$^+$). The neutral polymer P1 was synthesized by Suzuki coupling of 4,4'-(2,2-bis(4-((6-bromohexyl)oxy)phenyl)ethene-1,1-diyl)bis(bromobenzene) with 1,3-(2,5-dibromothiophen-3-yl)-2,5,8,11-tetraoxatridecane in 68% yield. P1 was then reacted with trimethylamine to yield the cationic conjugated polymer P1$^+$ (Scheme S1). The detailed synthetic procedures and characterization data are given in the Electronic Supplementary Information (ESI). The GPC analysis shows that the weight-average molecular weight (M_w) of P1 is 48337 g mol^{-1} and the polydispersity is 2.28. The presence of flexible *n*-octyl groups should have ameliorated the solubility of the polymer, which reduces the precipitation in the reaction process, and thus, enhances the molecular weight of the polymer. Although the molecular weight is high, P1$^+$ possesses excellent water solubility owing to the hydrophilic long chain ether groups on the thiophene units and the quaternary ammonium salt groups on the TPE units.

The absorption maximum of P1 is located at 367 nm (Fig. S1). P1 displays typical AIE characteristics, similar to previously reported TPE-containing polymers.[44,45] As shown in Fig. 1a-c, P1 possesses a good solubility in THF and shows weak emission at 498 nm with a fluorescence quantum yield (Φ_F) of 1.4% in THF. This is because its phenyl rings of the TPE moieties undergo active intramolecular

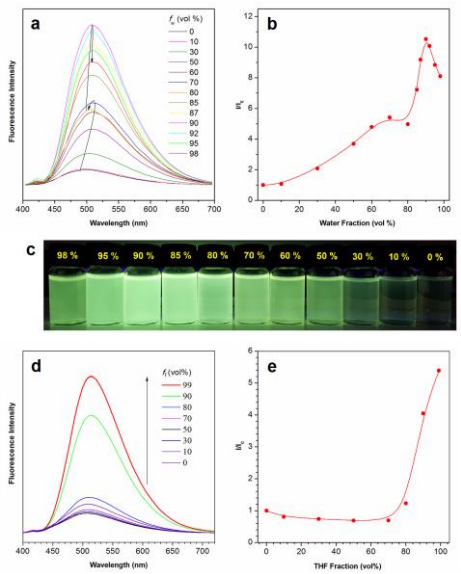

Fig. 1 (a) Fluorescence emission spectra of P1 in Water–THF mixtures with different water fractions. (b) Plot of relative PL intensity (I/I_0) versus the composition of the aqueous mixture of P1. (c) Photographs of P1 in THF solution and water–THF mixtures (water volume fraction from 0 to 98 %) taken under UV lamp illumination, (d) Fluorescence emission spectra of polyelectrolyte P1$^+$ in DMSO solution and DMSO–THF mixture. (e) Plot of relative PL intensity (I/I_0) versus the composition of DMSO–THF mixture of polyelectrolyte P1$^+$. Solution concentration: 10 μM; excitation wavelength: 370 nm.

Commented [WW2]: You need to highlight what is new with this work compared to published literature including your own work.

rotations in THF, which nonradiatively annihilates its excited state and makes it almost nonemissive.[46-49] However, with gradual addition of water, a poor solvent for P1, into THF, the resultant THF-water mixtures exhibit significantly enhanced emission with an increased Φ_F of 24.4% at a water fraction of 90 vol%. In solid film, P1 also gives a high Φ_F of 24.5%. The increase in Φ_F in both the THF/water mixture and the film is attributed to the hindrance of intramolecular rotation within P1, likely due to aggregation in the case of the solvent mixture and to either aggregation and/or the rotationally restricted environment within the film. This restriction of the intramolecular rotation (RIR) blocks the nonradiative decay channel, thus making the aggregates highly fluorescent. Therefore, the P1 indeed exhibits AIE properties.[48,49] The maximal emission peak at 508 nm is red-shifted by 10 nm when compared with that in solution, which is probably attributable to intermolecular interactions in the aggregate state.[50] The fluorescence decay profiles of P1 in THF and the THF/water mixture were not exponential (Fig. S2) but average lifetimes (τ_{AVE}) were computed, as per the equation $\tau_{AVE} = \Sigma f_i \tau_i$, (where f_i is the fractional contribution of the individual lifetime of each component (τ_i)).[51,52] The τ_{AVE} is enhanced from 0.189 ns to 1.112 ns with the addition of water into

the THF solution from zero to 90 vol% aqueous mixture, which is consistent with the observed changes in emission intensity.

The corresponding conjugated polymer P1$^+$ also exhibits AIE characteristics. P1$^+$ shows weak emission in DMSO, however, when a large amount of THF, a poor solvent for the P1$^+$, is added to the DMSO solution of P1$^+$ (f_{THF} >80 vol%), strong green emission is observed (Fig. 1d,e). P1 in the aggregated state not only has relatively stronger fluorescence intensity but also longer fluorescence lifetime. Thus, the large aggregation dependence of the time-resolved fluorescence decay process and Φ_F of P1$^+$ prompt us to explore the possibility of imaging the microstructures inside living cells with the CPE P1$^+$, as complementary method to traditional fluorescence intensity measurements.

P1$^+$ was assessed for its ability to interact with live mouse neuroblastoma neuro-2A cells using a confocal fluorescence microscope. After incubation with 5 μg mL^{-1} P1$^+$ for 30 min, the profile and microscopic structure of cells are clearly visible and bright green emission is observed (Fig. 2), suggesting P1$^+$ can enter and stain living cells easily. In particular, some P1$^+$ molecules are directly endocytozed by the cells and distributed in the cytoplasm, while others stay in the thin cytomembrane, so that the cells' round profile can be distinctly observed. The cytotoxicity of P1$^+$ was evaluated by the widely used MTT assay. The samples were

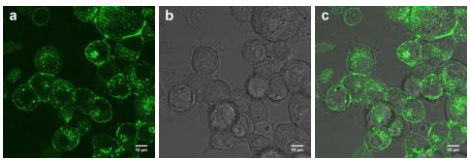

Fig. 2 Fluorescent images of mouse neuroblastoma neuro-2A cells stained with P1$^+$ (5 μg/mL) for 0.5 h at 37 °C. (a) fluorescence image, (b) bright field image, and (c) the overlay of fluorescence image and bright field image.

incubated with 0, 5, 10, 20 and 50 μM P1$^+$ for 24 hours, and at the highest concentration of 50 uM, the cell viability remains ~96%. This result suggests the water-soluble P1$^+$ has good biocompatibility (Fig. 3).

To further explore the density of P1$^+$ in the neuro-2A cells, the incubated cells were imaged using fluorescence lifetime imaging microscopy (FLIM) based on a TCSPC system. Owing to the large difference in the time-resolved fluorescent decay process of P1 at different molecular diffusion level, it is reasonable that P1$^+$ with

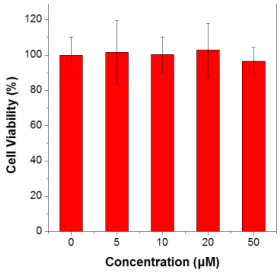

Fig. 3 Cytotoxicity of P1$^+$ on neuro-2A cells determined by MTT assay.

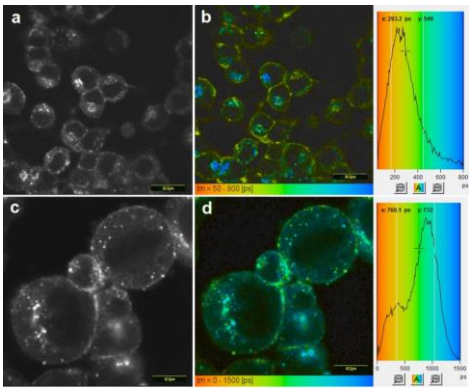

Fig. 4 Fluorescence lifetime images of mouse neuroblastoma neuro-2A cells stained with P1$^+$ (5 μg/mL for a and b; 20 ug/mL for c and d) for 0.5 h at 37 °C.

higher density in the cells should display longer fluorescence lifetime as well. FLIM images of the neuro-2A cells incubated with P1$^+$ are shown in Fig. 4, by applying a color scale from short (indicated by red color) to long (indicated by blue color) lifetimes. These images reveal that P1$^+$ is a highly suitable imaging probe for directly visualizing the cells' morphology, and more importantly, we can observe that the P1$^+$ remaining in the cytomembrane shows shorter lifetimes while that entering into the cells exhibits longer lifetimes. The lifetime histograms suggest that more P1$^+$ molecules stay in the cytomembrane rather than entering into the cells under low concentration conditions. Increasing the incubation concentration, leads to more P1$^+$ molecules being endocytozed by the cells and located inside the cells. The color distribution of the images supports the hypothesis that P1$^+$ molecules are inclined to aggregate in the central areas of cells rather than the cytomembrane. Long fluorescence lifetime areas in cells indicate the molecular motions slow down, probably due to aggregation or high viscosity in these regions.

Conclusions

In this work, we have designed and synthesized a neutral TPE-containing polymer P1, which is quaternized to afford a polyelectrolyte P1$^+$. P1$^+$ possesses excellent water solubility and shows AIE characteristics and strong green emission in the aggregated state. P1$^+$ is biocompatible and exhibits good performance in labeling mouse neuroblastoma neuro-2A cells as revealed by CLSM and TCSPC-based FLIM techniques. The results from FLIM images support the hypothesis that P1$^+$ molecules are inclined to aggregate in the central areas of cells exhibiting longer fluorescence lifetimes, while those staying on the cytomembrane are aggregated loosely associated with shorter fluorescence lifetimes. The molecular motion of P1$^+$ in cells can be monitored, providing information about aggregation or environmental viscosity as a function of location in cells. As such, we believe that this work could open a new avenue in the field of tracking the cancer cells

using AIE PCEs through both the CLSM and TCSPC-based FLIM technology.

Acknowledgements

We acknowledge the financial support from the National Natural Science Foundation of China (21404029, 21344007 and 21673082), the China Scholarship Council (201409645002), the Guangdong Natural Science Funds for Distinguished Young Scholar (2014A030306035), Scientific Research Fund of Zhejiang Provincial Education Department (Y201121319), Zhejiang Provincial Natural Science Foundation of China (LY14E30009) and the Fundamental Research Funds for the Central Universities (2017ZDPT001).

Notes and references

1 X. Duan, L. Liu, F. Feng and S. Wang, *Acc. Chem. Res.*, 2010, **43**, 260–270.
2 A. Duarte, K. Pu, B. Liu and G. C. Bazan, *Chem. Mater.*, 2011, **23**, 501–515.
3 X. Zhu, S. Guo, T. He, S. Jiang, D. Janczewski and G. J. Vancso, *Langmuir*, 2016, **32**, 1338–1346.
4 C. J. Arias, R. L. Surmaitis and J. B. Schlenoff, *Langmuir*, 2016, **32**, 5412–5421.
5 J. You, T. Park, J. Kim, J. S. Heo, H. Kim, H. O. Kim and E. Kim, *ACS Appl. Mater. Interfaces*, 2014, **6**, 3305–3311.
6 A. K. Dwivedi and P. K. Lyer, *J. Mater. Chem. B*, 2013, **1**, 4005–4010.
7 R. Zhan, A. J. H. Tan and B. Liu, *Polym. Chem.*, 2011, **2**, 417–421.
8 R. Liu, Y. Tan, C. Zhang, J. Wu, L. Mei, Y. Jiang and C. Tan, *J. Mater. Chem. B*, 2013, **1**, 1402–1405.
9 C. Nie, C. Zhu, L. Feng, F. Lv, L. Liu and S. Wang, *ACS Appl. Mater. Interfaces*, 2013, **5**, 4549–4554.
10 G. Yang, H. Yuan, C. Zhu, L. Liu, Q. Yang, F. Lv and S. Wang, *ACS Appl. Mater. Interfaces*, 2012, **4**, 2334–2337.
11 J. You, J. Kim, T. Park, B. Kim and E. Kim, *Adv. Funct. Mater.*, 2012, **22**, 1417–1424.
12 B. Bao, L. Yuwen, X. Zhan and L. Wang, *J. Polym. Sci., Part A: Polym. Chem.,* 2010, **48**, 3431–3439.
13 P. Zhang, H. Lu, H. Chen, J. Zhang, L. Liu, F. Lv and S. Wang, *Anal. Chem.*, 2016, **88**, 2985–2988.
14 M. Li, S. Li, H. Chen, R. Hu, L. Liu, F. Lv and S. Wang, *ACS Appl. Mater. Interfaces*, 2016, **8**, 42–46.
15 A. Parthasarathy, H. Ahn, K. D. Belfield and K. S. Schanze, *ACS Appl. Mater. Interfaces*, 2010, **2**, 2744–2748.
16 Y. Liu, P. Wu, J. Jiang, J. Wu, Y. Chen, Y. Tan, C. Tan and Y. Jiang, *ACS Appl. Mater. Interfaces*, 2016, **8**, 21984–21989.
17 R. Hu, H. Yuan, B. Wang, L. Liu, F. Lv and S. Wang, *ACS Appl. Mater. Interfaces*, 2014, **6**, 11823–11828.
18 H. Yuan, H. Chong, B. Wang, C. Zhu, L. Liu, Q. Yang, F. Lv and S. Wang, *J. Am. Chem. Soc.*, 2012, **134**, 13184–13187.
19 H. Chong, C. Nie, C. Zhu, Q. Yang, L. Liu, F. Lv and S. Wang, *Langmuir*, 2012, **28**, 2091–2098.
20 C. Tan, E. Atas, J. G. Muller, M. R. Pinto, V. D. Kleiman and K. S. Schanze, *J. Am. Chem. Soc.*, 2004, **126**, 13685-13694.
21 H. Jiang, P. Taranekar, J. R. Reynolds and K. S. Schanze, *Angew. Chem. Int. Ed.*, 2009, **48**, 4300-4316.
22 K. Pu, K. Li, J. Shi and B. Liu, *Chem. Mater.*, 2009, **21**, 3816–3822.
23 K. Pu, J. Shi, L. Cai, K. Li and B. Liu, *Biomacromolecules*, 2011, **12**, 2966–2974.
24 Y. Hong, J. W. Y. Lam and B. Z. Tang, *Chem. Commun.*, 2009, 4332–4353.
25 J. Mei, N. L. C. Leung, R. T. K. Kwok, J. W. Y. Lam and B. Z. Tang, *Chem. Rev.*, 2015, **115**, 11718–11940.
26 J. Liang, B. Z. Tang and B. Liu, *Chem. Soc. Rev.*, 2015, **44**, 2798–2811.
27 M. Gao, C. K. Sim, C. W. T. Leung, Q Hu, G. Feng, F. Xu, B. Z. Tang and B. Liu, *Chem. Commun.,* 2014, **50**, 8312–8315.
28 Y. Hong, L. Meng, S. Chen, C. W. T. Leung, L. Da, M. Faisal, D. Silva, J. Liu, J. W. Y. Lam, X. Huang and B. Z. Tang, *J. Am. Chem. Soc.*, 2012, **134**, 1680-1689.
29 C. W. T. Leung, Y. Hong, S. Chen, E. Zhao, J. W. Y. Lam and B. Z. Tang, *J. Am. Chem. Soc.*, 2013, **135**, 62–65.
30 Y. Yu, C. Feng, Y. Hong, J. Liu, S. Chen, K. M. Ng, K. Q. Luo and B. Z. Tang, *Adv. Mater.*, 2011, **23**, 3298–3302.
31 R. Hu, N. L. C. Leung and B. Z. Tang, *Chem. Soc. Rev.*, 2014, **43**, 4494–4562.
32 Z. Wang, S. Chen, J. W. Y. Lam, W. Qin, R. T. K. Kwok, N. Xie, Q. Hu and B. Z. Tang, *J. Am. Chem. Soc.*, 2013, **135**, 8238–8245.
33 X. Zhang, X. Zhang, B. Yang, J. Hui, M. Liu, Z. Chi, S. Liu, J. Xu and Y. Wei, *Polym. Chem.*, 2014, **5**, 683–688.
34 H. Lu, F. Su, Q. Mei, Y. Tian, W. Tian, R. H. Johnson and D. R. Meldrum, *J. Mater. Chem.*, 2012, **22**, 9890–9900.
35 Y. Chen and A. Periasamy, *Microsc. Res. Tech.*, 2004, **63**, 72–80.
36 P. Sarder, D. Maji and S. Achilefu, *Bioconjugate Chem.,* 2015, **26**, 963–974.
37 M. Y. Berezin and S. Achilefu, *Chem. Rev.*, 2010, **110**, 2641–2684.
38 M. Roding, S. J. Bradley, M. Nyden and T. Nann, *J. Phys. Chem. C*, 2014, **118**, 30282–30290.
39 X. Hao, L. J. McKimmie and T. A. Smith, *J. Phys. Chem. Lett.*, 2011, **2**, 1520–1525.
40 T. G. Terentyeva, J. Hofkens, T. Komatsuzaki, K. Blank and C. Li, *J. Phys. Chem. B*, 2013, **117**, 1252–1260.
41 C. M. Roth, P. I. Heinlein, M. Heilemann and D. P. Herten, *Anal. Chem.*, 2007, **79**, 7340–7345.
42 E. Derivery, C. Seum, A. Daeden, S. Loubery, L. Holtzer, F. Julicher and M. Gonzalez-Gaitan, *Nature*, 2015, **528**, 280–285.
43 S. Chen, Y. Hong, Y. Zeng, Q. Sun, Y. Liu, E. Zhao, G. Bai, J. Qu, J. Hao and B. Z. Tang, *Chem. Eur. J.*, 2015, **21**, 4315–4320.
44 Y. Wu, J. Shi, B. Tong, J. Zhi and Y. Dong, *Acta Polym. Sin.*, 2012, **12**, 1482–1490.
45 B. Xu, X. Wu, H. Li, H. Tong and L. Wang, *Polymer*, 2012, **53**, 490–494.
46 Y. Hong, J. W. Y. Lam and B. Z. Tang, *Chem. Commun.*, 2009, 4332–4353.
47 M. Wang, G. Zhang, D. Zhang, D. Zhu and B. Z. Tang, *J. Mater. Chem.*, 2010, **20**, 1858–1867.
48 J. Liu, J. W. Y. Lam and B. Z. Tang, *Chem. Rev.*, 2009, **109**, 5799–5867.
49 Y. Hong, J. W. Y. Lam and B. Z. Tang, *Chem. Soc. Rev.*, 2011, **40**, 5361–5388.
50 R. Hu, E. Lager, A. Aguilar-Aguilar, J. Liu, J. W. Y. Lam, H. H. Y. Sung, I. D. Williams, Y. Zhong, K. S. Wong, E. Pena-Cabrera and B. Z. Tang, *J. Phys. Chem. C*, 2009, **113**, 15845–15853.
51 G. Saito, J. A. Swanson and K. D. Lee, *Adv. Drug Delivery Rev.*, 2003, **55**, 199–215.
52 P. S. Pramod, N. U. Deshpande and M. Jayakannan, *J. Phys. Chem. B,* 2015, **119**, 10511–10523.

Commented [WW3]: As with the introduction, the main selling point of this work (compared to published literature) needs to be highlighted.

i.e. good solubility, better image contrast, etc.